

RESEARCH

Open Access



Brain-wide mapping of c-Fos expression in nitroglycerin-induced models of migraine

Shaobo Xiao^{1,2,4†}, Guangshuang Lu^{1,2,5†}, Jiayi Liu^{1,2†}, Wenjie Su^{1,2}, Chenhao Li^{1,2}, Yingyuan Liu^{1,2}, Fanchao Meng^{1,2}, Jinjing Zhao⁶, Nan Gao^{2,3}, Yan Chang^{1,2}, Xinghao Guo^{1,2}, Shengyuan Yu^{1,2*} and Ruozhuo Liu^{1,2*}

Abstract

Background Migraine is a neurological disorder characterized by complex, widespread, and sudden attacks with an unclear pathogenesis, particularly in chronic migraine (CM). Specific brain regions, including the insula, amygdala, thalamus, and cingulate, medial prefrontal, and anterior cingulate cortex, are commonly activated by pain stimuli in patients with CM and animal models. This study employs fluorescence microscopy optical sectioning tomography (fMOST) technology and AAV-PHPeB whole-brain expression to map activation patterns of brain regions in CM mice, thus enhancing the understanding of CM pathogenesis and suggesting potential treatment targets.

Methods By repeatedly administering nitroglycerin (NTG) to induce migraine-like pain in mice, a chronic migraine model (CMM) was established. Olcegepant (OLC) was then used as treatment and its effects on mechanical pain hypersensitivity and brain region activation were observed. All mice underwent mechanical withdrawal threshold, light-aversive, and elevated plus maze tests. Viral injections were administered to the mice one month prior to modelling, and brain samples were collected 2 h after the final NTG/vehicle control injection for whole-brain imaging using fMOST.

Results In the NTG-induced CMM, mechanical pain threshold decreased, photophobia, and anxiety-like behavior were observed, and OLC was found to improve these manifestations. fMOST whole-brain imaging results suggest that the isocortex-cerebral cortex plate region, including somatomotor areas (MO), somatosensory areas (SS), and main olfactory bulb (MOB), appears to be the most sensitive area of activation in CM ($P < 0.05$). Other brain regions such as the inferior colliculus (IC) and intermediate reticular nucleus (IRN) were also exhibited significant activation ($P < 0.05$). The improvement in migraine-like symptoms observed with OLC treatment may be related to its effects on these brain regions, particularly SS, MO, ansiform lobule (AN), IC, spinal nucleus of the trigeminal, caudal part (Sp5c), IRN, and parvicellular reticular nucleus (PARN) ($P < 0.05$).

[†]Shaobo Xiao, Guangshuang Lu and Jiayi Liu contributed equally to this work.

*Correspondence:
Shengyuan Yu
yusy1963@126.com
Ruozhuo Liu
liuruozhuo301@163.com

Full list of author information is available at the end of the article

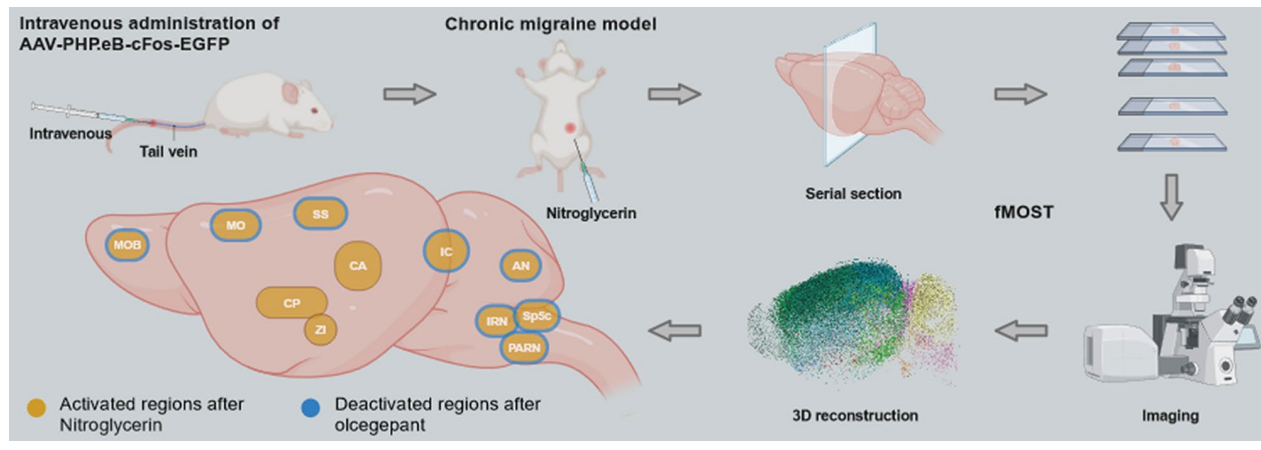


© The Author(s) 2024. **Open Access** This article is licensed under a Creative Commons Attribution-NonCommercial-NoDerivatives 4.0 International License, which permits any non-commercial use, sharing, distribution and reproduction in any medium or format, as long as you give appropriate credit to the original author(s) and the source, provide a link to the Creative Commons licence, and indicate if you modified the licensed material. You do not have permission under this licence to share adapted material derived from this article or parts of it. The images or other third party material in this article are included in the article's Creative Commons licence, unless indicated otherwise in a credit line to the material. If material is not included in the article's Creative Commons licence and your intended use is not permitted by statutory regulation or exceeds the permitted use, you will need to obtain permission directly from the copyright holder. To view a copy of this licence, visit <http://creativecommons.org/licenses/by-nc-nd/4.0/>.

Conclusions fMOST whole-brain imaging reveals c-Fos+ cells in numerous brain regions. OLC improves migraine-like symptoms by modulating brain activity in some brain regions. This study demonstrates the activation of the specific brain areas in NTG-induced CMM and suggests some regions as a potential treatment mechanism according to OLC.

Keywords Chronic migraine, Fluorescence micro-optical sectioning tomography, Calcitonin gene-related peptide, C-fos, Neural circuits, Olcegepant

Graphical Abstract



Background

Migraine is a neurological disorder characterized by complex, widespread, and sudden attacks [1]. Chronic migraine (CM) affects 1–2% of the population and develops from episodic migraine at a rate of approximately 3% per year [2]. However, its pathogenesis remains unclear. Recent neuroimaging studies in patients with CM have identified brain structures that are coactivated by pain stimuli, including the insula, amygdala, thalamus, and cingulate cortex [3]. Similarly, in chronic migraine models (CMMs) induced by chronic intraperitoneal injection of nitroglycerin (NTG) and repeated dural application of inflammatory soup, activation in brain areas, such as the medial prefrontal cortex (mPFC), anterior cingulate cortex (ACC), and caudal part of the spinal trigeminal nucleus (Sp5c) was observed [4].

In humans, migraine can be triggered by different compounds, such as nitric oxide (NO) donor NTG and calcitonin gene-related peptide (CGRP). NTG leads to elevated levels of intracellular cyclic guanosine monophosphate (cGMP) while CGRP leads to increased intracellular cyclic adenosine monophosphate (cAMP). The activation of cAMP and cGMP pathways ultimately triggers the opening of ATP-sensitive potassium (K_{ATP}) channels. Therefore, the modulation of nociceptive transmission through K_{ATP} channels may serve as a central pathway in the initiation of a migraine attack [5, 6]. The administration of NTG causes migraine-like symptoms in animals that closely resemble those experienced by humans and also increases the sensitivity of the structures involved in migraine pathophysiology [7].

Gepants, CGRP receptor antagonists, have been proven to be successful in both treating acute migraine attacks and preventing them [8]. In models of migraine induced by NTG, selective CGRP receptor antagonists like olcegepant (OLC) have shown to alleviate mechanical pain threshold in the hind paw and periorbital area by reducing brain activation [4]. Nevertheless, the majority of previous studies have examined particular areas of the brain and have yielded inconsistent findings through conventional approaches [9].

Gaining insights into neural activity across the entire brain is essential for comprehending how the brain functions and malfunctions. Fluorescence micro-optical sectioning tomography (fMOST), which utilizes a microtome, light microscope, and image recorder, enables rapid visualization of neurons by fluorescent labelling [10, 11]. AAV-PHP.eB, a highly permeable variant of the AAV serotype 9 that can cross the blood-brain barrier effectively, has been employed for comprehensive brain transduction [12]. The combination of AAV-PHP.eB with fMOST will accelerate observational studies that encompass the entire brain. In this research, we utilized fMOST to chart the evolving activation of brain regions in mice with mimic features of CM, while also investigating c-Fos, an immediate-early gene often utilized in mapping brain activity. The protein product of Fos gene expression has been used as an important marker of neuronal activation and the immunohistochemical method is widely used to identify specific brain regions whose activities are altered by stimuli [13].

Methods

Animals

The study's sample size was determined based on previous research [14]. Specific pathogen-free male C57BL/6 mice (aged 8–10 weeks, weighted 20–30 g) were obtained from SiPeiFu Biotechnology Co., Ltd. in Beijing, China. The mice were kept in a controlled environment with temperatures between 22 and 26 °C, humidity levels of 40–60%, a 12-hour light/dark cycle, and provided with unlimited food and water. Mice were left to acclimatize for 1 week prior to starting experiments. For behavior, the sample size was calculated by G*Power (ver. 3.1.9.7) based on the repeated measures design ($\alpha=0.05$, power=0.80, effect size=0.25) and the results showed the total sample size was 27, that means 9 mice per group. In our study, the sample size for behavior was 10 mice per group [15]. All procedures involving the animals were approved by the Institutional Animal Care and Use Committee of the Chinese People's Liberation Army (PLA) General Hospital, and conducted following the Regulations for the Administration of Affairs Concerning Experimental Animals.

Experimental protocol and groups

Part I

Mice ($n=10$ per group) were randomized into CMM, OLC treatment, and control (CON) groups. CMM was induced by the intraperitoneal injection of NTG. The OLC treatment group was administered the drug prior to NTG administration, whereas the CON group was administered the vehicle control (VEH). After modeling each group, all mice were subjected to the mechanical

withdrawal threshold (MWT), light-aversive test (LAT), and elevated plus maze (EPM) tests (Fig. 1).

Part II

Three groups of mice ($n=3$ per group) were randomly assigned to the CMM, OLC treatment, and CON groups. All three groups of mice received AAV injections one month before the CM experiment. The CM experiment was continued for 9 days. Two hours after the last NTG/VEH injection to establish the CMM, the mice were sacrificed and subjected to whole-brain imaging with fMOST (Fig. 1).

The total number of mice used in the study was 39. The animals were assigned to the experimental group using a randomized program (<http://www.randomizer.org/>).

Establishment of the chronic migraine model

The CM model was established as described previously. NTG (Beijing Yi Ming, Beijing, China) was prepared from a stock solution of 5.0 mg/ml NTG in 30% alcohol, 30% propylene glycol, and 0.9% saline. The administration of NTG involved a meticulous dilution process to achieve a concentration of 1 mg/ml in 0.9% saline before injection. The intraperitoneal method was used to administer NTG at a dose of 10 mg/kg every other day for nine consecutive days. The VEH contained 0.9% saline, 6% propylene glycol, and 6% alcohol and the method of administration was the same as that of NTG. The dosage regimen was based on findings from credible literature sources [16, 17].

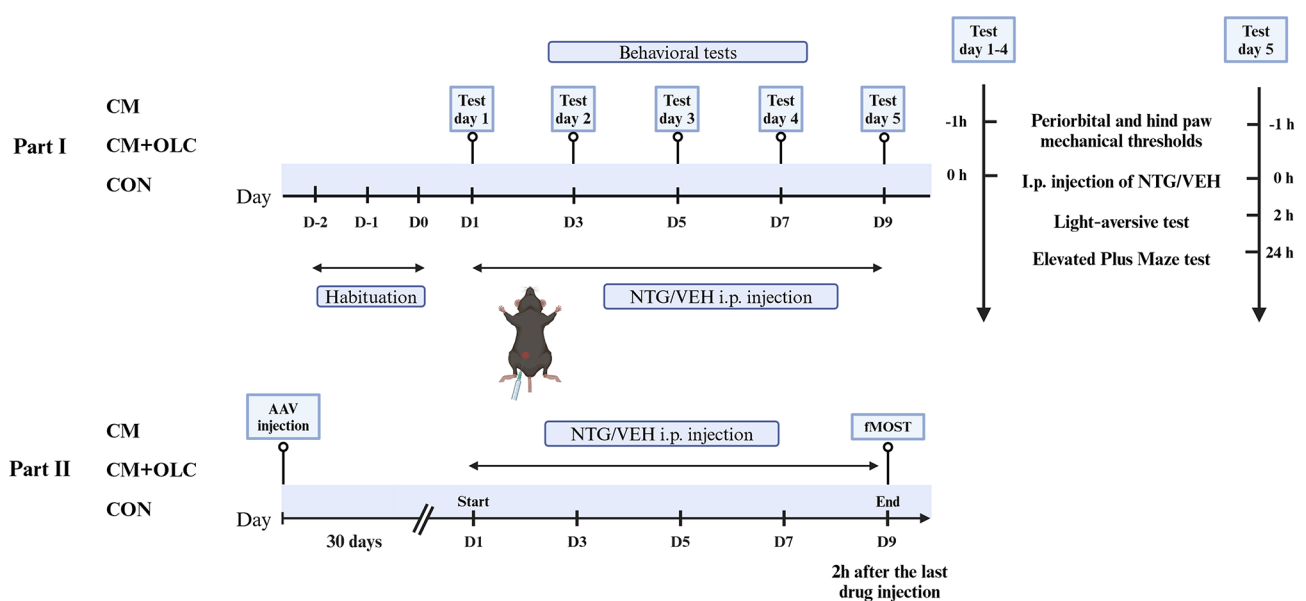


Fig. 1 Experimental protocol and groups. (Created with BioRender.com)

Drug administration

OLC compound, obtained from MedChemExpress (HY-10095), was dissolved in dimethyl sulfoxide (DMSO) to reach a concentration of 5 mg/mL. In preparation for injection, the OLC solution was diluted with 0.9% saline using an ultrasonic instrument to a concentration of 0.1 mg/mL. Following this, OLC was given intraperitoneally at a dosage of 1 mg/kg 15 min prior to NTG injection [18, 19]. In the NTG-induced migraine model, 2% DMSO+0.9% saline was used as the VEH. Using this combination, we established a baseline for our study and accurately measured the effects of the interventions. The mice were randomly divided into three groups: (1) CM, (2) CM+OLC, and (3) CON.

Behavioral tests

In order to guarantee accurate and unbiased results, the mice were familiarized with the behavior room in advance to reduce any possible stress factors. The behavior room was described as quiet and clean, with adequate lighting, proper ventilation, and no noticeable smells. All behavioral tests were conducted consistently at a set time every day from 9:00 AM to 4:00 PM. Furthermore, the same batch of mice was used for all behavioral experiments to manage any external factors. The same experimenter was used throughout the behavioral tests. The experimenter was not aware of the experimental groups in advance.

Mechanical withdrawal threshold (MWT) test

The von Frey filament test was conducted to measure MWT, utilizing filaments ranging from 0.008 g to 2 g. Before administering NTG or vehicle, the mice's periorbital and hind paw thresholds were evaluated. The exact thresholds were determined using a novel statistical algorithm through the up-down method. The process started with a weight of 0.16 g, where a negative response (O) led to an increase in stimulus weight and a positive response (X) led to a decrease, maintaining a minimum interval of 30 s between stimuli. Once the breaking point (OX/XO) was reached, four more stimuli were administered to establish a specific response pattern. These patterns and the resulting filaments were recorded, and withdrawal thresholds were calculated using a free online algorithm available at https://bioapps.shinyapps.io/von_frey_app/ [20].

Each mouse was placed individually in a clear plastic chamber measuring 8 cm × 15 cm to assess the hind paws. The chamber was positioned on a wire mesh grid, and the mice were allowed at least 30 min to acclimate daily for a minimum of three days before testing. This test involves the application of von Frey filaments perpendicular to the plantar surface of the hind paw. A positive response was considered if the mouse exhibited

brisk paw withdrawal, flinching, lifting, or licking during stimulation or immediately after filament removal. Each mouse was tested on a small disk (5 cm diameter) placed 30 cm horizontally for the periorbital assessment. For three consecutive days before measurements, the mice were acclimated to the disks for 30 min each day. The periorbital region, from the lower eyelid to the midline, was subjected to thorough testing. A positive response was indicated by the mouse vigorously stroking its face with its paws on the same side, shaking its head, or retracting its head from the stimulus.

Light-aversive test (LAT)

To assess the light aversion behavior of mice, a light-dark box (30 cm wide × 15 cm deep × 30 cm high) was used to evaluate the typical photophobia associated with migraine induced by NTG. The evaluation took place 2 h after injecting either NTG or a placebo on the last day of testing. The light-dark box from Shanghai Xinruan Information Technology Co., Ltd. (model XR-XB120, Shanghai, China) was divided into two identical sections: one was illuminated with bright white light (1000 lx) from an LED panel, while the other remained dimly lit and painted black (<5 lx). The two compartments were separated by an open channel (7×7 cm) to allow the mice to move freely. In this study, we investigated light-aversive behavior in several groups of mice during the 110–130 min phases after NTG/VEH injection. Our methodology was based on a previous field [21, 22]. Every mouse was placed precisely in the middle of the illuminated section, with its back turned towards the darker part. The container was meticulously sanitized using 75% alcohol. The movement patterns were captured on video and assessed using Supermaze software. Metrics such as total distance covered, transitions between chambers, and time spent in each chamber were all meticulously calculated.

Elevated plus maze (EPM) test

Anxiety and mood disorders are commonly seen as psychiatric conditions that often coexist with migraines [23]. Previous research has documented anxiety-related behaviors, particularly in animal models of CM [24, 25]. This study focused on measuring the level of anxiety in a CMM induced by NTG using an EPM test. We utilized the EPM (Shanghai Xinruan Information Technology Co., Ltd., XR-XG201, Shanghai, China) to assess anxiety-like behavior associated with migraine. The maze was elevated 60 cm above the ground and comprised two open arms (35 cm wide, 5 cm deep, 60 lx) and two enclosed arms (35 cm wide, 5 cm deep, 15 cm high, <5 lx) connected by a central platform (5 cm wide, 5 cm deep). Mice were placed on the central platform, facing one of the open arms, and were given 10 min to freely

explore the EPM. The maze was thoroughly cleaned with 75% alcohol, and SuperMaze software (Shanghai Xinruan Information Technology Co., Ltd., XR-Xmaze, Shanghai, China) was employed to monitor and analyze their movements, including the time spent in the open and closed arms and the frequency of entries into each. The EPM test was conducted on separate groups of mice 24 h after the NTG/VEH injection.

AAV viruses and viral injections

The AAV vector, rAAV-PHP.eB-cFos-EGFP, was employed to label the c-Fos protein in the entire brain (supplied by Brain Case Biotechnology Co., Ltd). The vector can cross the blood-brain barrier. The viral stock samples were determined to have titers of 5.78×10^{12} viral genomes/ml and were securely stored at -80 degrees Celsius. rAAV-PHP.eB-cFos-EGFP was injected one month prior to the CM experiment in three CMM mice, three OLC-treated mice, and three CON mice. The mice were administered a dose of 1.156×10^{11} viral genomes per mouse in 100 μ l of sterile phosphate-buffered saline (PBS) through the lateral caudal vein.

fMOST

Tissue preparation

The mice were rendered deeply unconscious with an intraperitoneal injection of 1.25% Avertin (a mixture of 12.5 mg/mL of 2,2,2-Tribromoethanol and 25 μ L/mL 2-Methyl-2-butanol, Sigma, T48402, 152463, St. Louis, MO, USA) at a dose of 0.2 ml/10 g body weight. Following this, they were perfused through the heart with a solution of 4% paraformaldehyde (PFA) and 0.01 M PBS. Their brains were then carefully removed and fixed in 4% PFA for 24 h at 4 °C. A 3–5% agarose powder solution was prepared using distilled water. Post-fixing mouse brains were embedded in an agarose solution and carefully positioned. The samples were then left undisturbed for 8–10 min until the agarose solution solidified.

Whole-brain imaging

The procedure for preparing the fMOST samples in this study followed a protocol similar to a previous study [11]. Before imaging, a whole-brain sample from the mouse was fixed in place in the anteroposterior direction on a 3D translation stage and positioned in a water bath containing 0.01 M PBS. The sample was then placed in a solution to achieve a consistent refractive index for the objective lens during imaging, with the PBS aiding in enhancing EGFP fluorescence. The imaging process adopted a tomographic approach, where each image had a thickness of 40 μ m. The process involved four key steps: (1) vibrating sectioning using a specially designed vibratome with a vibration frequency of 77 Hz and a cutting speed of 0.2 mm/s along the x-axis. (2) moving the

platform to the initial position for imaging. (3) conducting light sheet scanning imaging. (4) repositioning the platform to the cutting tool setup point ready for the next layer of imaging. Images obtained from fMOST were analyzed using the BioMapping 9000 system (Oebio Biological Co., Ltd., Wuhan, China) [26].

Image processing

All the acquired images were preprocessed for one detection channel. This process involved performing a lateral illumination correction for each stripe and stitching the stripes together based on their spatial orientation and overlap. Thereafter, the data were down-sampled to match the average template of the Common Coordinate Framework version 3 (CCFv3). To achieve accurate registration, down-sampling was conducted within the Brain Registration, Identification, and Encoding Framework (BRIEF) interface. This pipeline facilitates cell quantification in different regions by employing interactive 3D cell detection, precise cell categorization with a convolutional neural network (CNN), and identifying cell positions within the annotation.

Brain-wide c-Fos expression analysis

C-Fos expression in the mouse brain was analyzed at the level of individual cells using the brain-wide c-Fos fMOST method, which examines 253 anatomical regions in the mouse brain. The results are presented as bar graphs showing the distribution of c-Fos expression across different brain regions.

Statistical analysis

The data were presented as the mean plus or minus the standard error of the mean (S.E.M.). Analysis was carried out using SPSS version 27 (IBM Analytics, Armonk, N.Y., USA) for various statistical tests including the two-tailed unpaired Student's t-test, one-way ANOVA, and repeated-measures ANOVA. Data were further examined using repeated-measures analysis of variance (ANOVA), with subsequent post-hoc tests utilizing Bonferroni or Fisher's least significant difference (LSD). GraphPad Prism (version 10, GraphPad Software, Inc., San Diego, CA, USA) was utilized for data visualization. The results of each analysis were included in a numerical legend, with statistical significance considered at $P < 0.05$.

Results

CM-like Phenomenology of the NTG-Induced Migraine Model in mice

In order to create the CMM model, NTG was given every other day for 9 days, with OLC given 15 min before NTG in the treatment groups. During the modeling phase, the mice were assessed for mechanical pain threshold, photophobia, and anxiety-like behaviors. Mechanical pain

threshold tests were performed before each NTG or VEH injection, and the Light Aversive Test (LAT) and Elevated Plus Maze (EPM) test were performed 2 and 24 h after the last injection, respectively. Mechanical threshold tests were performed before each NTG or VEH injection, while the LAT and EPM tests were performed 2 and 24 h after the last injection, respectively. Compared with the CON group and CM+OLC group, the mechanical thresholds of the hind paw in the CM group were significantly lower ($n=10/\text{group}$, 3d, 5d, 7d, 9d: $P<0.001$; Fig. 2B). and periorbital region. Equally, compared with the CON group and CM+OLC group, the mechanical thresholds of the hind paw in the CM group were significantly lower ($n=10/\text{group}$, CON vs. CM, 3d, 5d, 7d, 9d: $P<0.001$, CM+OLC vs. CM, 3d: $P<0.01$, 5d: $P<0.01$, 7d: $P<0.05$, 9d: $P<0.01$).

In addition to assessing mechanical thresholds, we quantified the anxiety levels in NTG-induced CMM using the EPM test. We found that the time spent in the open arm ($n=10/\text{group}$, CON vs. CM, $P<0.001$, CM+OLC vs. CM, $P<0.05$; Fig. 2F) and the number of open arm entries ($n=10/\text{group}$, CON vs. CM, $P<0.001$, CM+OLC vs. CM, $P=0.084$; Fig. 2H) in the CM group were further reduced. Meanwhile, the time spent in the closed arms increased ($n=10/\text{group}$, CON vs. CM, $P<0.001$, CM+OLC vs. CM, $P=0.061$; Fig. 2G) and closed-arm entries reduced ($n=10/\text{group}$, CON vs. CM, $P<0.01$; CM+OLC vs. CM, $P=0.073$; Fig. 2I).

Finally, photophobia was assessed using a modified light/dark box. CM mice spent significantly less time in light than CON and CM+OLC mice for a total of 20 min ($n=10/\text{group}$, CON vs. CM, CM+OLC vs. CM, $P<0.001$; Fig. 2K, M). Analysis of transitions between the light and dark chambers revealed no signs of photophobia in CM mice compared to the other two groups ($n=10/\text{group}$, CON vs. CM, $P=0.294$; CM+OLC vs. CM, $P=0.074$; Fig. 2L).

Whole brain expression distribution of c-Fos positive cells in Nitroglycerin-Induced models of Migraine

c-Fos+cells have been detected in up to 220 different brain regions. (Fig. 3, Videos 1–3). In the CON group, the top 25 brain regions with over 2000 cFos+cells comprised somatosensory areas (SS), somatomotor areas (MO), visual areas (VIS), retrosplenial area (RSP), and the main olfactory bulb (MOB), simple lobule (SIM), caudoputamen (CP), anterior cingulate area (ACA), Ammon's horn (CA), ansiform lobule (AN), inferior colliculus (IC), central lobule (CENT), culmen (CUL), orbital area (ORB), auditory areas (AUD), entorhinal area (ENT), agranular insular area (AI), anterior olfactory nucleus (AON), piriform area (PIR), declive (DEC), subiculum (SUB), intermediate reticular nucleus (IRN),

paraflocculus (PFL), prelimbic area (PL), medial vestibular nucleus (MV) (Fig. 4).

In the CM+OLC group, we identified the top 25 brain regions with more than 2000 c-Fos+cells, including the SS, MO, VIS, MOB, RSP, SIM, IC, CA, ACA, AN, CENT, ENT, CUL, CP, AUD, ORB, PIR, AI, AON, PFL, IRN, flocculus (FL), DEC, SUB, and midbrain reticular nucleus (MRN) (Fig. 4).

In the CM group, 29 brain regions had more than 2000 c-Fos+cells. The top 25 brain regions were SS, MO, MOB, VIS, RSP, AN, SIM, IC, CP, ACA, AON, CUL, ORB, CA, PIR, AUD, CENT, AI, ENT, DEC, IRN, PFL, lateral septal nucleus (LS), parvicellular reticular nucleus (PARN) and paramedian lobule (PRM) (Fig. 4).

Key brain regions displaying c-Fos expression difference in Nitroglycerin-Induced models of Migraine

Comparative analysis revealed statistically significant differences in c-Fos expression between the CM and CON groups, as well as between the CM and CM+OLC groups in the brains of mice. A total of 254 mouse brain regions were evaluated, and c-Fos+cells were present in 227 of these regions, with the most notable increase observed in the isocortical cerebral cortex plate (CTXpl) region. Comparison of the left, right, and total numbers of c-Fos+cells in each brain region revealed several statistically significant increases in the CM group compared to the CON group, notably the SS ($P<0.05$), MOB ($P<0.01$), IC ($P<0.0001$), IRN ($P<0.05$), and medullary reticular nucleus (MDRN) ($P<0.05$). In the left or right side-specific comparison between the CM group and the CON group, there was a statistically significant increase in the number of c-Fos+cells in regions such as MO ($P<0.01$), SS ($P<0.0001$), MOB ($P<0.001$), IC ($P<0.0001$), IRN ($P<0.001$), spinal nucleus of the trigeminal, caudal part (Sp5c) ($P<0.01$), MDRN ($P<0.05$), zona incerta (ZI) ($P<0.001$), PARN ($P<0.001$), AN ($P<0.05$), and CA ($P<0.05$).

Furthermore, comparisons between the CM group and the CM+OLC groups regarding the total number of c-Fos+cells revealed a statistically significant increase in MO ($P<0.05$), SS ($P<0.0001$), MOB ($P<0.05$), and CP ($P<0.001$). In the left or right side-specific comparison between the CM group and the CM+OLC group, there was a statistically significant increase in the number of c-Fos+cells in regions including MO ($P<0.01$), SS ($P<0.0001$), MOB ($P<0.001$), IC ($P<0.01$), IRN ($P<0.01$), Sp5c ($P<0.05$), PARN ($P<0.01$), AN ($P<0.01$), CP ($P<0.0001$), and ENT ($P<0.01$). These findings suggest that specific brain regions are differentially activated in mice with CM induced by NTG and that OLC treatment may modulate this activation. Future studies are warranted to further investigate the neurobiological mechanisms underlying these observations and their potential

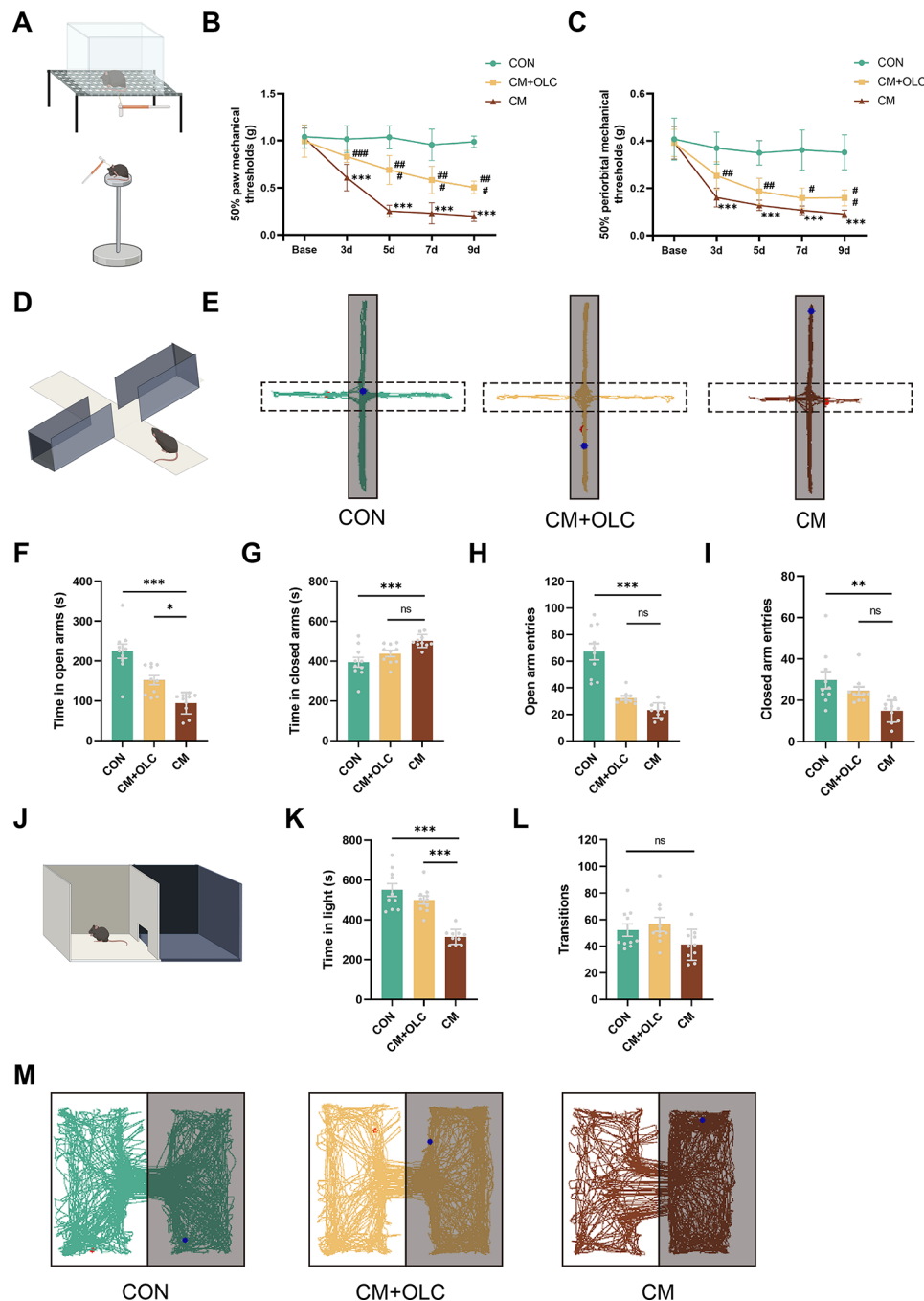


Fig. 2 Behavioral tests. **A-C** The basal mechanical pain thresholds of the hind paw and periorbital area during the injection of NTG. The data are presented as the mean \pm SEM. Two-way repeated-measures ANOVA with post hoc comparison. ($n=10$ per group, CM vs. CON, * $p < 0.05$, ** $p < 0.01$, *** $p < 0.001$, **** $p < 0.0001$; CM vs. CM + OLC, # $p < 0.05$, ## $p < 0.01$, ### $p < 0.001$, #### $p < 0.0001$) **D-I** Elevated Plus Maze test. Time in open arms (**F**), time in closed arms (**G**), open arm entries (**H**), and closed arm entries (**I**) were counted statistically. **J-M** Light-averse test. Time in light (**K**) and transitions (**L**) were analyzed statistically. The data are presented as the mean \pm SEM. One-way ANOVA with the Bonferroni post hoc test. ($n=10$ per group, ns: no significant difference, * $p < 0.05$, ** $p < 0.01$, *** $p < 0.001$, **** $p < 0.0001$) (Created with [BioRender.com](https://www.biorender.com))

implications in the treatment of CM and its comorbidities. Notably, brain regions such as MO, SS, MOB, CA, and ENT are all located in CTXpl. The IC is located in the midbrain and is sensory-related (MB-sen). The Sp5c is located at the medulla and is sensory-related (MY-sen).

IRN, MDRN, and PARN are located in the medulla and are motor-related (MY-mot). The ZI is located in the hypothalamic lateral zone (LZ). AN is located in the cerebellar cortex and hemispheric regions. The CP is located in the dorsal region.

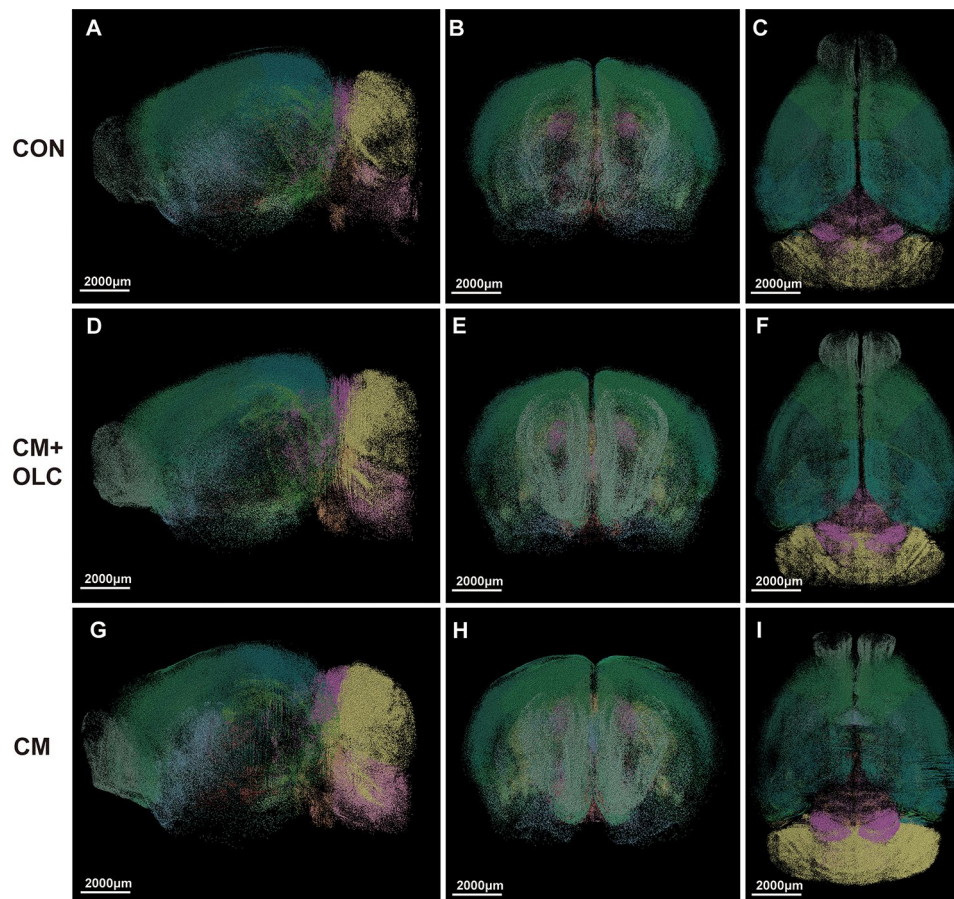


Fig. 3 The images of c-Fos mapping from a representative animal in each of the three groups (CON, CM+OLC, CM). (A, D, G) Sagittal plane; (B, E, H) Coronal plane; (C, F, I) Horizontal plane. Scale bar, 2000 μm

Somatosensory areas (SS)

The SS is located in the isocortex (Fig. 5A, C, D, and E). Generally, the number of c-Fos+cells in the SS of the CM group exceeded that of the CON group ($P < 0.01$) and CM+OLC group ($P < 0.0001$). Further analysis revealed that there was no statistically significant difference between the CM group and CON group in the left SS ($P = 1.000$), whereas the right SS of the CM group increased significantly ($P < 0.0001$) (Fig. 5B, F–K).

Main olfactory bulb (MOB)

The MOB is located in the isocortex (Fig. 6A, C, D, and E). Generally, the number of c-Fos+cells in the MOB of the CM group was greater than that of the CON group ($P < 0.01$) and the CM+OLC group ($P < 0.05$). Further analysis showed that there was no statistical difference between the CM group and CON group in the left MOB, whereas the right MOB of the CM group increased more than that of the CON group ($P < 0.001$) and CM+OLC ($P < 0.001$) (Fig. 6B, F–K).

Inferior colliculus (IC)

The IC is located in the midbrain and is sensory-related (MB-sen) (Fig. 7A, C, D, and E). Generally, the number of c-Fos+cells in the IC of the CM group exceeded that of the IC of the CON group ($P < 0.0001$). Further analysis showed that the left IC of the CM group increased more than that of the CON group ($P < 0.05$), while the right IC of the CM group increased more than that of the CON group ($P < 0.0001$) and CM+OLC ($P < 0.01$) (Fig. 7B, F–K).

Somatomotor Area (MO)

The MO is located in the isocortex (Fig. 8A, C, D, and E). In general, the number of c-Fos+cells in the MO was not significantly different from those in the CM group and CON group ($P = 0.862$). Further analysis showed that there was no statistical difference between the CM group and CON group in the left MO, whereas the right MO of the CM group increased more than that of the CON group ($P < 0.01$) and CM+OLC ($P < 0.01$) (Fig. 8B, F–K).

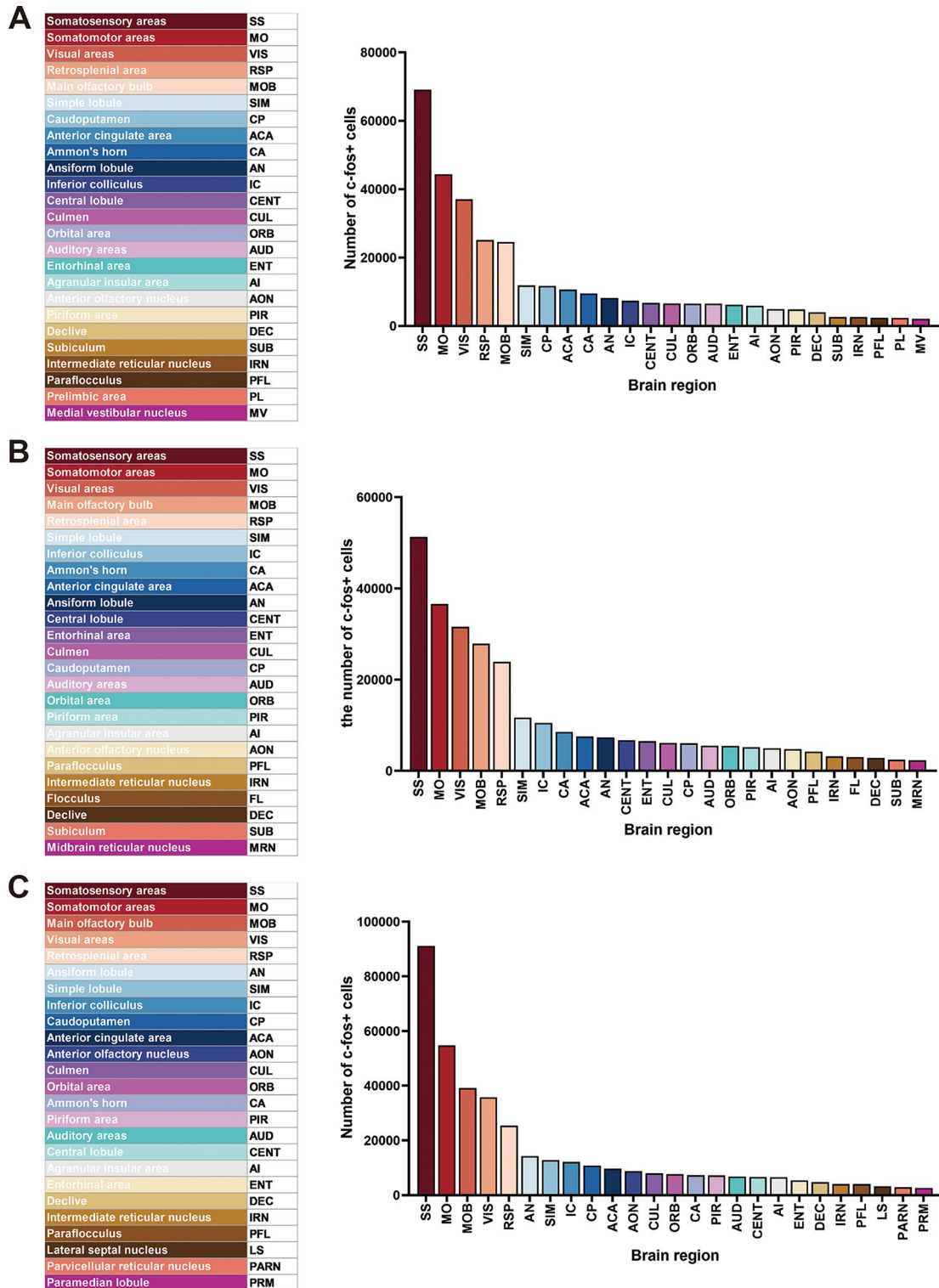


Fig. 4 The top 25 brain regions with more than 2000 c-Fos+ expressing cells in three groups. **(A)** CON group; **(B)** CM+OLC group; **(C)** CM group. Scale bar, 2000 μ m. ($n=3$)

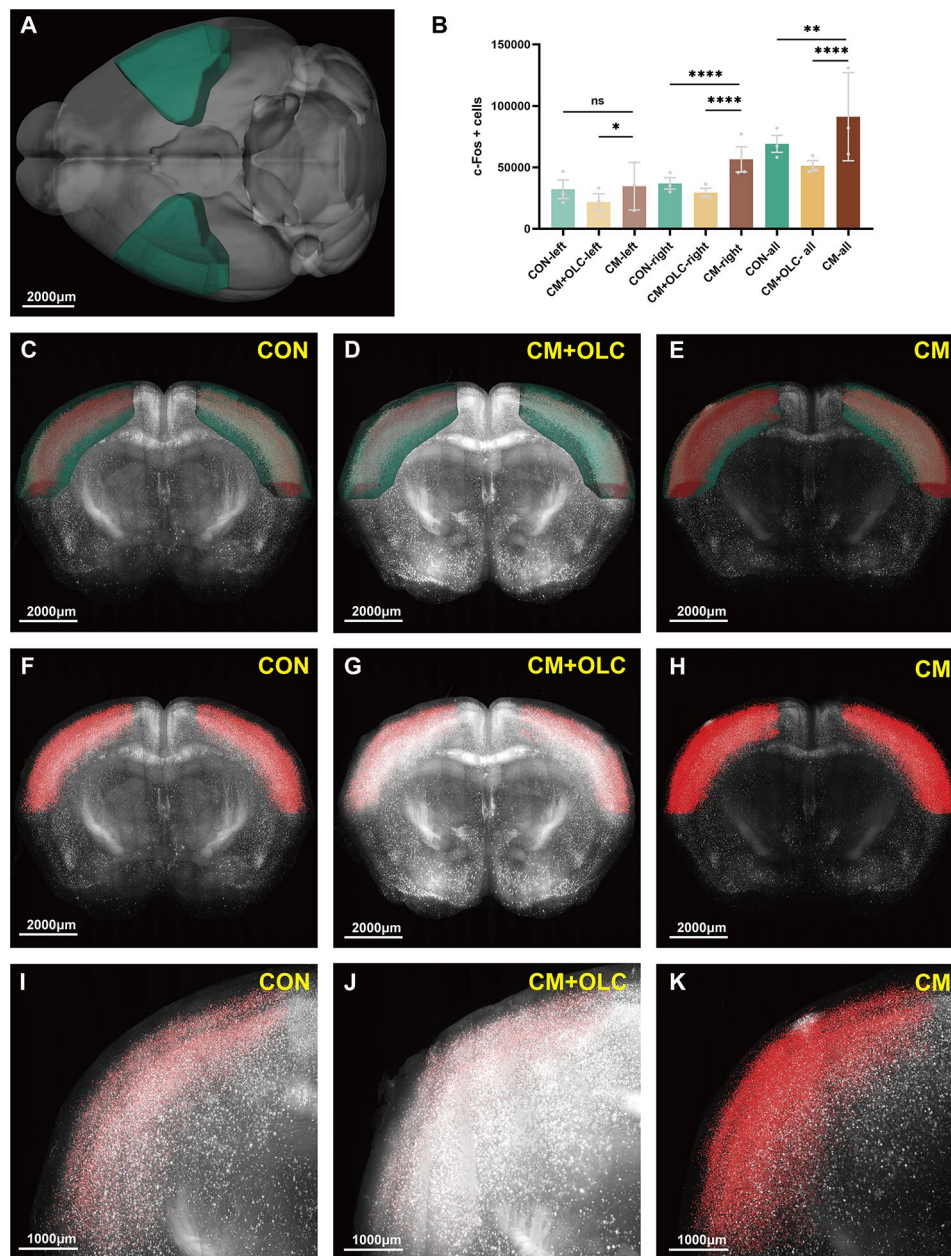


Fig. 5 The number of c-Fos+ expressing cells in the somatosensory areas (SS). (A, C, D, E) SS was located at the isocortex. Green marks the SS according to Allen Mouse Brain Common Coordinate Framework V3. (B, F, G, H) The number of c-Fos+ cells in the SS of the CM group was more than that of the CON group or the CM+OLC group. Red marks the c-Fos+ cells. (I, J, K) The enlarged view from (F, G, H). Scale bar: (A–H) 2000 μ m, (I, J, K) 1000 μ m. Two-tailed unpaired Student's t-test. Error bars indicate SEM. ($n=3$ per group, * $p<0.05$, ** $p<0.01$, *** $p<0.001$, **** $p<0.0001$)

Intermediate reticular nucleus (IRN)

The IRN is located in the medulla and is motor-related (MY-mot) (Fig. 9A, C–E). In general, the number of c-Fos+ cells in the IRN of the CM group was higher than that of the CON group ($P<0.05$). Further analysis showed that there was no statistical difference between the CM group and CON group in the left IRN, while the right IRN of the CM group increased more than that of the CON group ($P<0.001$) and CM+OLC ($P<0.01$) (Fig. 9B, F–K).

Spinal nucleus of the trigeminal, caudal part (Sp5c)

The Sp5c is located at the medulla and is sensory-related (MY-sen) (Figure S1 A, C–E). In general, the number of c-Fos+ cells in the Sp5c was not significantly different between the CM group and CON group ($P=0.7962$). Further analysis showed that there was no statistical difference between the CM group and CON group in the left Sp5c ($P=1.0000$), whereas the right Sp5c of the CM group increased more than that of the CON group ($P<0.01$) and CM+OLC ($P<0.05$) (Figure S1 B, F–K).

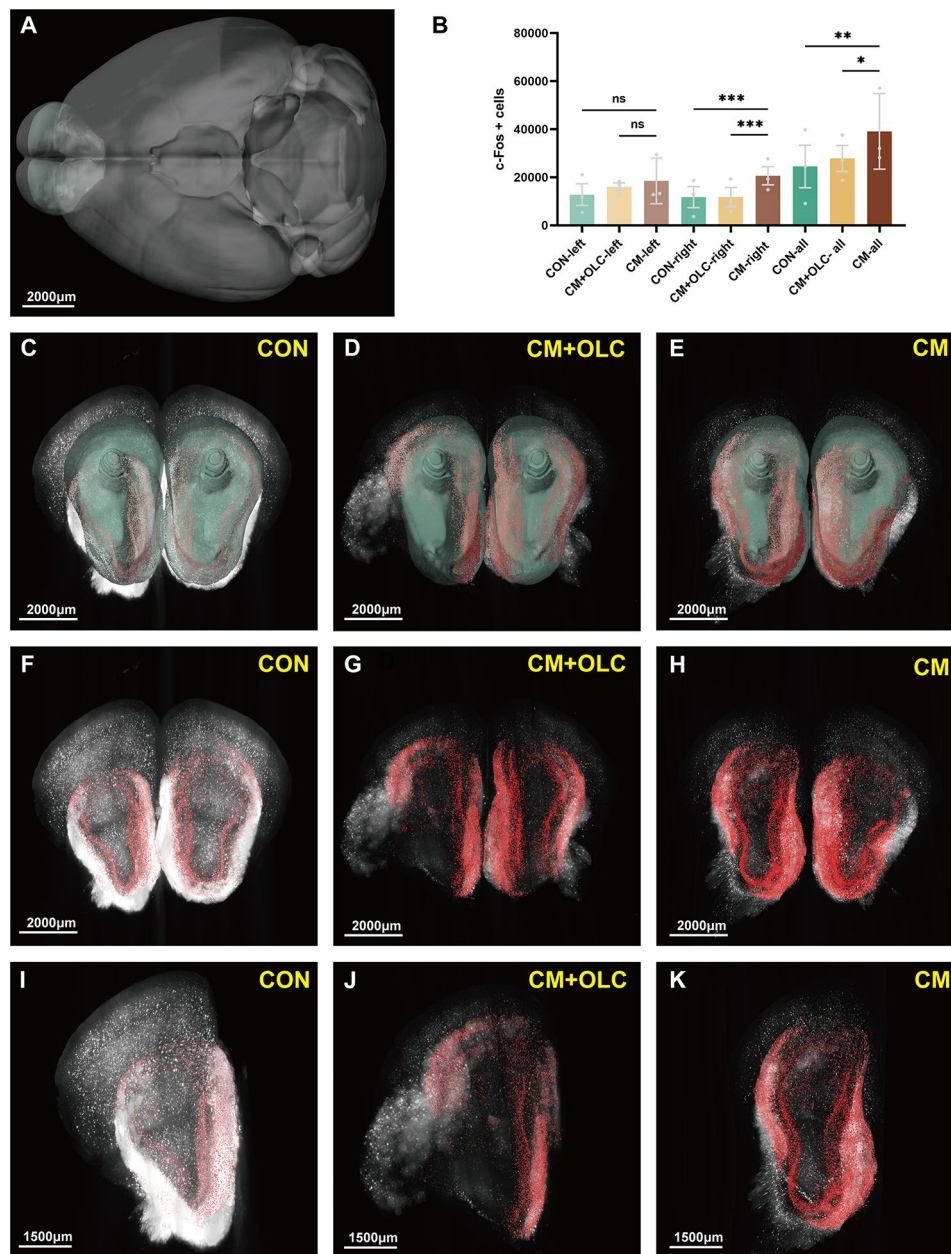


Fig. 6 The number of c-Fos+ expressing cells in the main olfactory bulb (MOB). (A, C, D, E) MOB was located at the isocortex. Green marks the MOB according to Allen Mouse Brain Common Coordinate Framework V3. (B, F, G, H) The number of c-Fos+ cells in the MOB of the CM group was more than that of the CON group or the CM+OLC group. Red marks the c-Fos+ cells. (I, J, K) The enlarged view from (F, G, H). Scale bar: (A–H) 2000 μ m, (I, J, K) 1500 μ m. Two-tailed unpaired Student's t-test. Error bars indicate SEM. ($n=3$ per group, * $p<0.05$, ** $p<0.01$, *** $p<0.001$, **** $p<0.0001$)

Parvicellular reticular nucleus (PARN)

PARN is located in the medulla and is motor-related (MY-mot) (Figure S2 A, C–E). In general, the number of c-Fos+ cells in the PARN was not significantly different from those in the CM group and CON group ($P=0.4050$). Further analysis showed that there was no statistical difference between the CM group and CON group in the left PARN ($P=1.0000$), whereas the right PARN of the CM group increased more than that of the CON group ($P=0.0004$) and CM+OLC ($P<0.01$) (Figure S2 B, F–K).

Ansiform lobule (AN)

The AN is located in the cerebellar cortex (Figure S3 A, C–E). As regards the number of c-Fos+ cells in the AN, there was no significant difference from those in the CM group and CON group ($P=0.8680$). Further analysis showed that there was no statistical difference between the CM group and CON group in the left AN ($P=1.0000$), while the right AN of the CM group increased more than that of the CON group ($P<0.05$) and CM+OLC ($P<0.01$) (Figure S3 B, F–K).

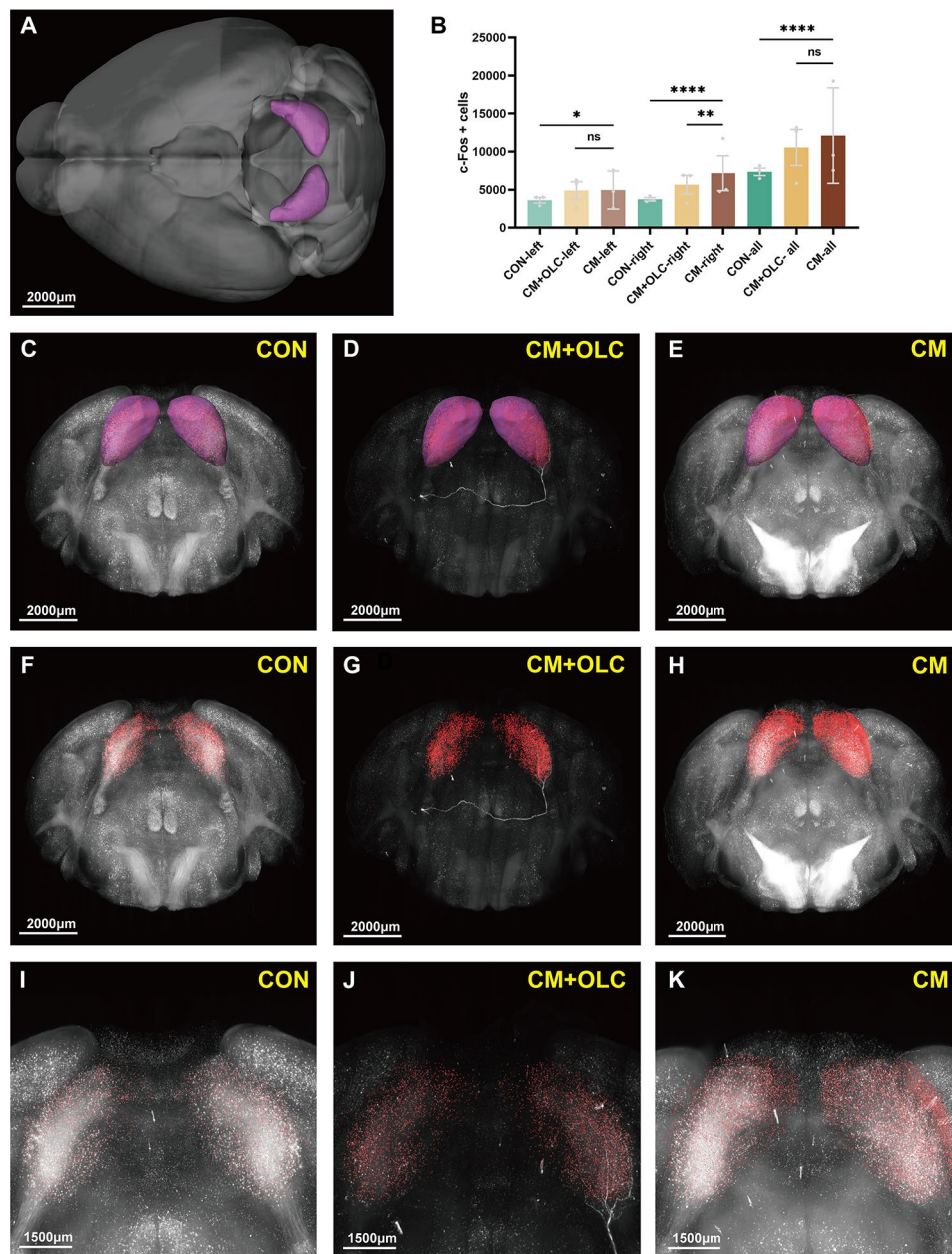


Fig. 7 The number of c-Fos+ expressing cells in the inferior colliculus (IC). (A, C, D, E) IC was located at the midbrain, sensory related (MB-sen). Pink marks the IC according to Allen Mouse Brain Common Coordinate Framework V3. (B, F, G, H) The number of c-Fos+ cells in the IC of the CM group was more than that of the CON group or the CM+OLC group. Red marks the c-Fos+ cells. (I, J, K) The enlarged view from (F, G, H). Scale bar: (A–H) 2000 μ m, (I, J, K) 1500 μ m. Two-tailed unpaired Student's t-test. Error bars indicate SEM. ($n=3$ per group, * $p < 0.05$, ** $p < 0.01$, *** $p < 0.001$, **** $p < 0.0001$)

Discussion

The current study investigated the cumulative effects of NTG-induced CM on the brain and behavior of mice and provided a comprehensive map of the brain regions activated by pain sensitization in mice. Leveraging the fMOST and AAV-PHP.eB techniques, we present a detailed map of the cumulative expression of c-Fos in the brain of an NTG-induced CM model, laying the groundwork for future research.

In CMMs, comprising repeated dural application of an inflammatory soup and chronic systemic injection of NTG, research on brain activation remains limited. Previous studies mainly analyzed changes in c-Fos expression in brain regions that may be associated with headaches after modelling [27–34]. A recent study found that in the NTG-induced CMM, c-Fos expression was significantly increased in the medial prefrontal cortex (mPFC), anterior cingulate cortex (ACC), and the caudal part of the spinal trigeminal nucleus (Sp5c) [4]. However,

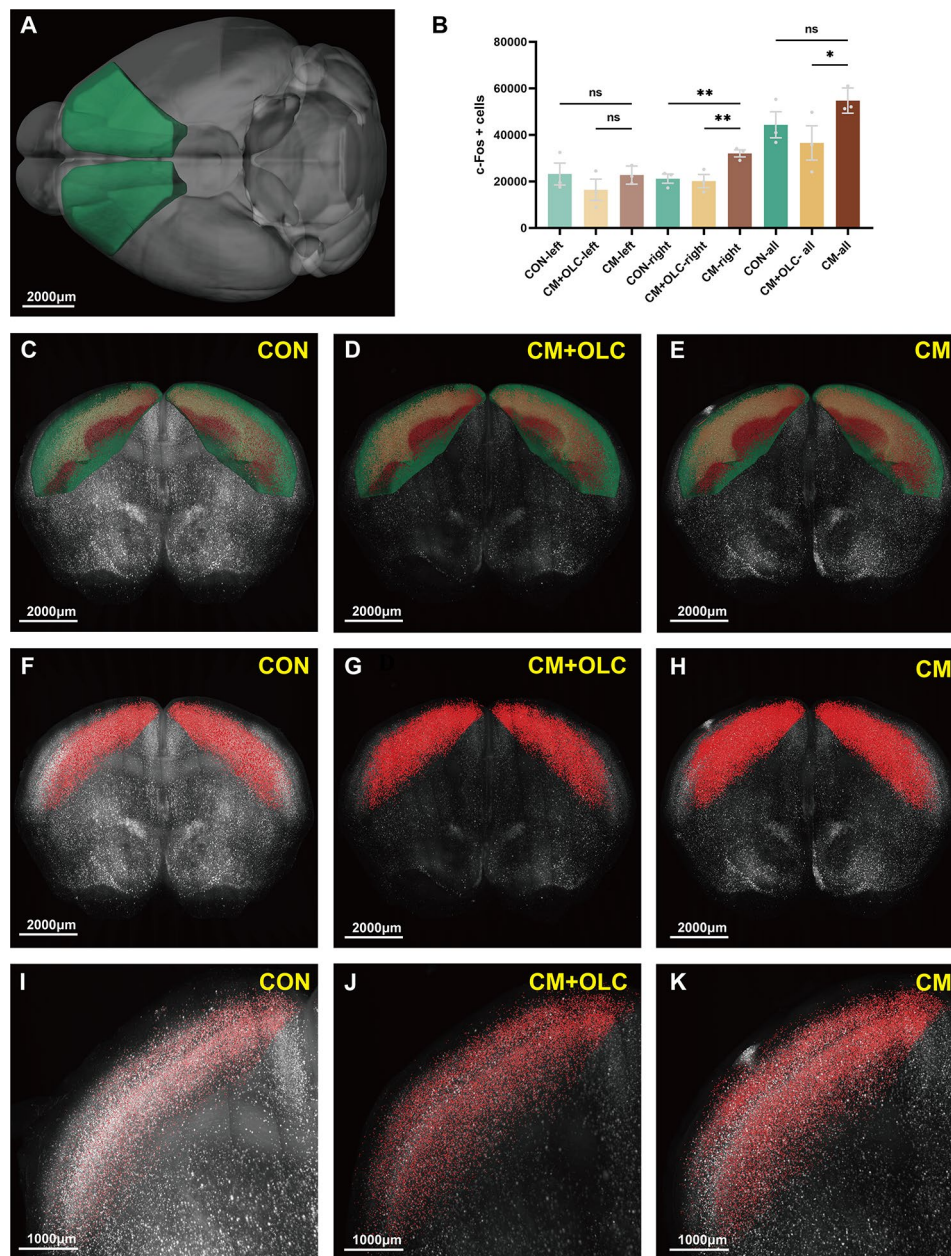


Fig. 8 The number of c-Fos+ expressing cells in the somatomotor area (MO). (A, C, D, E) MO was located at the isocortex. Green marks the MO according to Allen Mouse Brain Common Coordinate Framework V3. (B, F, G, H) The number of c-Fos+ cells in the MO of the CM group was more than that of the CON group or the CM+OLC group. Red marks the c-Fos+ cells. (I, J, K) The enlarged view from (F, G, H). Scale bar: (A–H) 2000 μ m, (I, J, K) 1000 μ m. Two-tailed unpaired Student's t-test. Error bars indicate SEM. ($n=3$ per group, * $p<0.05$, ** $p<0.01$, *** $p<0.001$, **** $p<0.0001$)

the study's focus was limited to only five representative coronal sections, which fell short of offering an accurate and comprehensive view of c-Fos mapping in the entire brain. Using neurotropic viruses, genes encoding fluorescent proteins can be introduced into the nervous system. Fluorescent labelling of specific types of neurons can be achieved by combining viral and recombinant enzyme systems. Additionally, real-time imaging with fMOST enables whole-brain distribution imaging of specific cell types [35]. Previous studies used the fMOST system to

map the whole-brain distribution of fluorescently labeled positive cells efficiently [36].

Our findings indicated that CM mice receiving repeated administrations of NTG developed persistent mechanical pain threshold decreased accompanied by notable photophobia and anxious behaviors, mirroring clinical manifestations observed in patients with migraine. Additionally, OLC alleviated hind paw and periorbital mechanical pain threshold, photophobia, and anxiety in these mice. We observed widespread activation

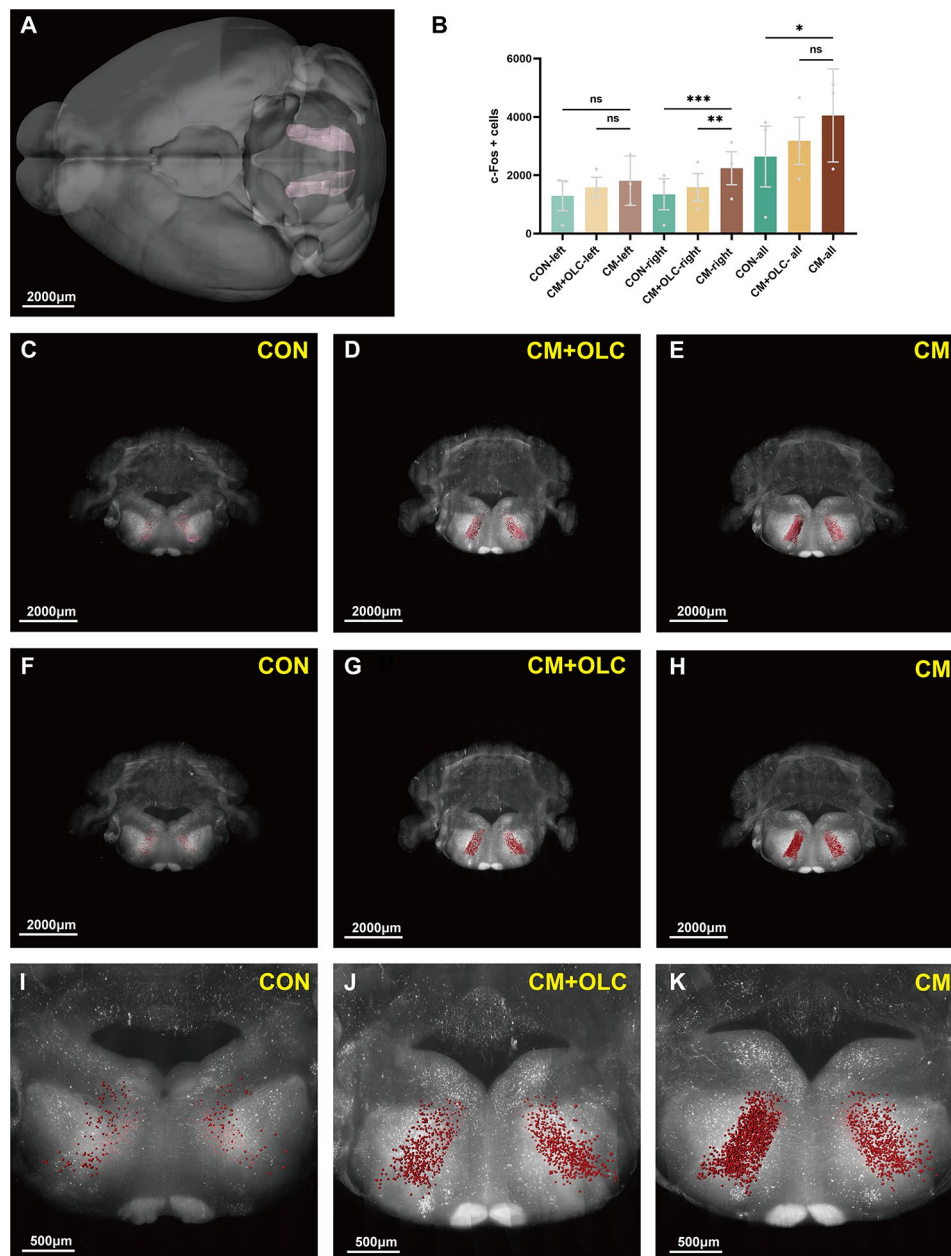


Fig. 9 The number of c-Fos+ expressing cells in the intermediate reticular nucleus (IRN). (**A, C, D, E**) IRN was located at the medulla, motor related (MY-mot). Pink marks the IRN according to Allen Mouse Brain Common Coordinate Framework V3. (**B, F, G, H**) The number of c-Fos+ cells in the IRN of the CM group was more than that of the CON group or the CM+OLC group. Red marks the c-Fos+ cells. (**I, J, K**) The enlarged view from (**F, G, H**). Scale bar: (A–H) 2000 μ m, (I, J, K) 500 μ m. Two-tailed unpaired Student's t-test. Error bars indicate SEM. ($n=3$ per group, $*p<0.05$, $**p<0.01$, $***p<0.001$, $****p<0.0001$)

of c-Fos in NTG-induced CMM, albeit with varying levels of expression across different brain regions. The expression patterns of c-Fos in diverse migraine models, based on published research, are summarized in Table 1. Furthermore, OLC diminished c-Fos activation in several brain regions, elucidating the effects of NTG and OLC treatment on brain activation.

Our study unveiled a notable activation pattern in the CTXpl region, characterized by an increased number of c-Fos+ cells in areas such as the MO, SS, and MOB.

Additionally, significant activation was observed in other brain regions, including the IC and IRN. We also found that there are differences in the lateralized expression of c-Fos in some brain regions, including the CA, Sp5c, PARN, and AN. Notably, the SS region exhibited significant activation. Brain function activation in primary headaches typically involves regions related to pain processing, such as the somatosensory areas, cingulate cortex, and thalamus [37, 38]. Furthermore, increased activation was observed in the MO area of the CTXpl

Table 1 The summarization of previous studies that focused on the expression of c-Fos in migraine animal models

Year	Journal	Animals	Stimuli methods	Test methods	Test level	Testing brain regions	Brain regions of significant increasing of c-fos
2023 [40]	International Journal of Molecular Sciences	mice	nitroglycerin-induced	Immunofluorescence	Proteins	Hypothalamus	A11 nucleus
2023 [41]	Frontiers in Molecular Neuroscience	rats	repeated dural infusion of IS	Immunofluorescence	Proteins	Brain stem	PAG
2022 [42]	Molecular Brain	mice	optogenetic induction of CSD	VISoR and Immunofluorescence	Proteins	Whole brain	Somatosensory, Primary sensory, Olfactory, Basal ganglia
2022 [4]	The Journal of Headache and Pain	mice	nitroglycerin/levcromakalim-induced	Immunofluorescence	Proteins	PVT, vIPAG, mPFC, ACC, Sp5c	mPFC, ACC, Sp5c
2020 [43]	Cephalalgia	mice	generation of E700K transgenic mice and CSD	Immunohistochemistry	Proteins	Bregma 0.7 mm Bregma -0.7 mm Bregma -1.6 mm	SS, PIR, STR, and amygdala
2019 [44]	Neural Regeneration Research	rhesus monkey	infusion of IS	Immunohistochemistry	Proteins	trigeminal nucleus caudalis, frontal lobe, parietal lobe, thalamus, hypothalamus, hippocampus, midbrain, pons, and the upper and lower segment of the medulla	TNC, thalamus, hypothalamus, midbrain and pons
2014 [45]	Cephalalgia	rats	intravenous CGRP administration	RT-PCR/ Immunohistochemistry	Proteins/ mRNA	Brain stem	NTS, CVLM
2013 [46]	Neurological Sciences	rats	electrical stimulation of the trigeminal ganglion	Immunohistochemistry	Proteins	Brain stem	NRM, TNC
2001 [47]	Cephalalgia	rats	intracisternal administration of the irritant capsaicin	Immunocytochemistry	Proteins	Hindbrain, Midbrain nuclei, Forebrain nuclei	TNC, LC, DR, VMH, PVH, SO

PAG, periaqueductal gray; CSD, cortical spreading depression; VISoR, volumetric imaging with synchronized on-the-fly-scan and readout; mPFC, medial prefrontal cortex; ACC, anterior cingulate cortex; Sp5c, caudal part of the spinal trigeminal nucleus; PVT, paraventricular thalamic nucleus; vIPAG, ventrolateral periaqueductal gray; IS, inflammatory soup; CFA, complete Freund's adjuvant; SS, somatosensory cortex; PIR, piriform cortex; STR, striatum; TNC, trigeminal nucleus caudalis; NTS, nucleus tractus solitarius; CVLM, caudal ventrolateral medulla; NRM, nucleus raphe magnus; LC, locus coeruleus; DR, dorsal raphe; PVH, paraventricular; VMH, ventromedial hypothalamic nucleus; SO, supraoptic

region. Previous studies have identified the motor cortex as a commonly targeted area for non-invasive neural stimulation, and motor cortex stimulation (MCS) is effective in the clinical treatment of chronic neuropathic pain [39]. Non-invasive neurostimulation has also opened up promising treatment prospects for migraine [40]. A recent study found that chronic activation of the M1 region of the motor cortex can significantly alleviate pain caused by von Frey filament mechanical stimulation and that the ZI and periaqueductal gray matter (PAG) regions were most activated during M1 region activation

[39]. Concurrently, we also observed significant activation in the ZI region, suggesting the existence of a top-down pain modulation process from the motor cortex to the ZI region during the development of CM. Eventually, migraine may progress to a chronic decompensated state, which requires further investigation.

CA, also known as the hippocampus, is involved in the regulation of cognition and memory. Clinical evidence suggests that cognitive symptoms in patients with migraine may stem from structural and functional abnormalities in the cerebral cortex, hippocampus, and

white matter [40]. Patients often adapt to adverse stress events during CM, which can induce structural and functional changes in the hippocampus [41]. In our study, we observed a significant activation in the right hippocampus. Previous studies have shown a positive correlation between the volume of the right hippocampus and a favorable prognosis in migraine, implying that the right hippocampus may be more active in chronic pain situations [42].

In this study, significant activation was observed in the MOB. Previous reports have indicated a relationship between odor and the trigeminal-nociceptive pathway in the pathophysiology of migraine [43]. Sleep disorders, anxiety, depression-like behaviors, and cognitive impairment are common comorbidities in patients with migraine. Previous studies have shown that the ENT is a key node connecting the hippocampus and certain neocortical and subcortical regions and is associated with depression-like behaviors [44]. The olfactory bulb transmits signals to the olfactory area of the cerebral cortex through the posterior end of the olfactory tract, which then reaches the ENT region. In this study, both the hippocampus and MOB showed significant activation, suggesting the possible involvement of the entorhinal-hippocampal neural network in the regulation of depression-like behaviors and mild cognitive impairment in CM [45].

With the development of functional MRI (fMRI), studies on brain function changes in patients with migraine without aura have revealed reduced volumes in several brain regions, including the bilateral superior and inferior colliculi, PAG, locus coeruleus, MRN, and dorsal pontine medullary junction [46]. In this study, significant activation was observed in the IC, located in a sensory-related region of the midbrain and is typically associated with hearing. Patients with migraine often experience auditory hypersensitivity, known as phonophobia, although its cause and localization remain unclear [47].

Additionally, significant activation of second-order neurons was observed in the Sp5c, a sensory-related brain region located in the medulla, which is consistent with previous studies [4]. Recently, the activation of microglia and neuroinflammation leading to central sensitization in the Sp5c region of mice with CM induced by NTG has also been reported [48, 49]. The activation of the SS, Sp5c, and midbrain regions is consistent with previous studies and further confirms the involvement of the activation and sensitization of the trigeminal vasculo-neural pathway in the pathophysiology of migraine [50]. Both IRN and PARN are located in the motor-related region of the medulla oblongata and are important nuclear groups of the reticular formation. The lateral reticular formation mainly receives fibers from all sensory pathways, such as somatosensory fibers from the

spinal trigeminal and principal nuclei or olfactory fibers through the medial forebrain bundle. Combined with this study, the co-activation of the SS, Sp5c, MOB, and reticular formation seems to explain the functional connections of some migraine-related clinical manifestations.

After NTG intervention, we observed significant activation in certain brain regions, which then showed a marked decrease following OLC treatment. Specifically, regions such as the MO, SS, MOB, IC, Sp5c, IRN, PARN, and AN exhibited notable reductions in activation after OLC therapy, whereas MDRN and ZI did not show significant decreases. CGRP receptors are widely expressed in the rodent brain, and the discovery of CGRP receptor elements, namely calcitonin receptor-like receptor and receptor activity-modifying protein 1, has propelled advancements in this field [51, 52]. Currently, CGRP are believed to be present in various regions, including the cortex, thalamus, amygdala, periaqueductal gray matter, locus coeruleus, trigeminal nucleus caudalis, parabrachial nucleus, hypothalamus, and cerebellum [53]. In our study, the brain regions that showed a significant decrease in activation after the OLC intervention included SS and MO in the cerebral cortex, AN in the cerebellar cortex, and IC, Sp5c, IRN, and PARN in the brainstem. These regions, notably activated after NTG intervention, may be involved in the pathogenesis of CM. The significant reduction in activation observed after OLC treatment suggests that OLC's ability to improve migraine-like symptoms in mice is related to these brain regions. Current research suggests that Gepants primarily act on peripheral CGRP receptors, with their impact on the central nervous system still being unclear. Our study results indicate that Gepants may also have an effect on the central nervous system, although the specific mechanisms are not yet understood. Of course, there is also the possibility that the therapeutic effects of olcegepant may be due to peripheral actions that secondarily influence central nervous system activity. This could involve modulation of sensory input from the periphery that affects the CNS regions implicated in migraine. Further in-depth research is needed in the future to explore the mechanisms by which gepants affect the central nervous system.

Limitations of the study

While this study serves as a foundation for future circuit research by utilizing fMOST technology to map c-Fos activation in brain regions of an NTG-induced CMM, it has some limitations. Firstly, the sample size was relatively small, resulting in poor reproducibility in some brain regions. Although there were trends compared to the control group, the differences were not statistically significant. Secondly, regarding the method of adenovirus-mediated whole-brain expression, there have been

precedents for whole-brain expression of c-Fos in previous studies, making this research more reliable. However, the identified brain regions require further validation by immunofluorescence. Thirdly, in our study, we indeed lacked a comparative study where only OLC was administered, which is a limitation. Although the mouse model established by administration of NTG can partially mimic human migraine attacks, the current findings in mice cannot be extended to humans. Lastly, taking into account the influence of female hormones on migraine-related pain processing, our experiments were conducted on male mice. Nevertheless, given that migraines predominantly affect females, the study's findings do not encompass the contribution of female hormones.

Conclusions

In this study, mice with NTG-induced CM exhibited mechanical pain threshold decreased, photophobia, and anxiety. Utilizing fMOST technology, we observed an increase in c-Fos expression in multiple brain regions of these mice. These findings indicate that the CTXpl region, including the MO, SS, and MOB, is the most sensitive area for activation in CM. Additionally, other brain regions, such as the IC and IRN, also displayed significant activation. The improvement in migraine-like symptoms observed with OLC treatment may be related to its effects on these brain regions, particularly the SS, MO, AN, IC, Sp5c, IRN, and PARN. The comprehensive brain activation maps generated in this study will provide valuable insights for future studies. Understanding the functional differences among various brain regions in mice with NTG-induced CM can offer insights into the treatment of CM and its comorbidities. This information may lead to the development of targeted therapies that address the specific neurobiological mechanisms underlying these conditions.

Abbreviations

ACA	Anterior cingulate area
ACC	Anterior cingulate cortex
AI	Agranular insular area
AN	Ansiform lobule
AON	Anterior olfactory nucleus
AUD	Auditory areas
CA	Ammon's horn
CENT	Central lobule
CGRP	Calcitonin gene-related peptide
CM	Chronic migraine
CMM	Chronic migraine model
CON	Control group
CP	Caudoputamen
CTXpl	Isocortex-cerebral cortex plate
CUL	Culmen
DEC	Declive
ENT	Entorhinal area
EPM	Elevated plus maze
FL	Flocculus
fMOST	Fluorescence micro-optical sectioning tomography
IC	Inferior colliculus
IRN	Intermediate reticular nucleus

LAT	Light-aversive test
LS	Lateral septal nucleus
LZ	Hypothalamic lateral zone
MDRN	Medullary reticular nucleus
MO	Somatomotor areas
MOB	Main olfactory bulb
mPFC	Medial prefrontal cortex
MRN	Midbrain reticular nucleus
MV	Medial vestibular nucleus
MWT	Mechanical withdrawal threshold
NTG	Nitroglycerin
OLC	Olcegepant
ORB	Orbital area
PAG	Periaqueductal grey
PARN	Parvicellular reticular nucleus
PFL	Paraflocculus
PIR	Piriform area
PL	Prelimbic area
PRM	Paramedian lobule
RSP	Retrosplenial area
SIM	Simple lobule
Sp5c	The caudal part of the spinal trigeminal nucleus
SS	Somatosensory areas
STRd	Striatum dorsal region
SUB	Subiculum
VEH	Vehicle control
VIS	Visual areas
ZI	Zona incerta

Supplementary Information

The online version contains supplementary material available at <https://doi.org/10.1186/s10194-024-01837-9>.

Supplementary Material 1: Supplemental figures

Supplementary Material 2: Video 1. CON group

Supplementary Material 3: Video 2. CM+OLC group

Supplementary Material 4: Video 3. CM group

Acknowledgements

We would like to express our gratitude to our laboratory members for their valuable discussions and technical assistance during the experiments. S. B. Xiao, G. S. Lu and J. Y. Liu contributed equally to this work. Some of the clipart icons appearing in Figs. 1 and 2 and figure in the visual abstract were created with BioRender (<https://biorender.com>).

Author contributions

S.X., G.L., and J.L. contributed equally to this work. R.L., and S.Y. designed and supervised the study. S.X., G.L., J.L., W.S., C.L., Y.L., F.M., J.Z., N.G., Y.C., and X.G. performed experiments and acquired data. S.X., G.L., and J.L. analyzed data. S.X., and J.L. wrote the paper. All authors read and approved the final manuscript.

Funding

The present study was funded by the Key Research and Development Program Project of the Ministry of Science and Technology (2023YFC2508702).

Data availability

No datasets were generated or analysed during the current study.

Declarations

Ethics approval and consent to participate

All animal experiments performed in this study were approved by the Institutional Animal Care and Use Committee of the Chinese PLA General Hospital and followed the Regulations for the Administration of Affairs Concerning Experimental Animals.

Consent for publication

Not applicable.

Competing interests

The authors declare no competing interests.

Author details

¹Medical School of Chinese PLA, Beijing 100853, China

²Department of Neurology, International Headache Center, The First Medical Center of Chinese PLA General Hospital, Fuxing Road 28, Haidian District, Beijing 100853, China

³School of Medicine, Nankai University, Tianjin 300071, China

⁴920th Hospital of Joint Logistics Support Force of People's Liberation Army of China, Kunming 650100, Yunnan, China

⁵Department of Pediatrics, The Lu'an Hospital Affiliated to Anhui Medical University, The Lu'an People's Hospital, Lu'an 237005, China

⁶Department of Neurology, The 305 Hospital of the People's Liberation Army, Beijing 100017, China

Received: 12 June 2024 / Accepted: 31 July 2024

Published online: 21 August 2024

References

- Jensen R, Stovner LJ (2008) Epidemiology and comorbidity of headache. *Lancet Neurol* 7(4):354–361. [https://doi.org/10.1016/S1474-4422\(08\)70062-0](https://doi.org/10.1016/S1474-4422(08)70062-0)
- May A, Schulte LH (2016) Chronic migraine: risk factors, mechanisms and treatment. *Nat Rev Neurol* 12(8):455–464. <https://doi.org/10.1038/nrneuro.2016.93>
- Lee MJ, Park BY, Cho S, Kim ST, Park H, Chung CS (2019) Increased connectivity of pain matrix in chronic migraine: a resting-state functional MRI study. *J Headache Pain* 20(1):29. <https://doi.org/10.1186/s10194-019-0986-z>
- Wu S, Ren X, Zhu C, Wang W, Zhang K, Li Z et al (2022) A c-Fos activation map in nitroglycerin/levcromakalim-induced models of migraine. *J Headache Pain* 23(1):128. <https://doi.org/10.1186/s10194-022-01496-8>
- Al-Karagholi MA, Ghanizada H, Nielsen CAW, Hougaard A, Ashina M (2021) Opening of ATP sensitive potassium channels causes migraine attacks with aura. *Brain* 144(8):2322–2332. <https://doi.org/10.1093/brain/awab136>
- Ashina M, Hansen JM, BO AD, Olesen J (2017) Human models of migraine - short-term pain for long-term gain. *Nat Rev Neurol* 13(12):713–724. <https://doi.org/10.1038/nrneuro.2017.137>
- Demartini C, Greco R, Zanaboni AM, Sances G, De Icco R, Borsook D et al (2019) Nitroglycerin as a comparative experimental model of migraine pain: from animal to human and back. *Prog Neurobiol* 177:15–32. <https://doi.org/10.1016/j.pneurobio.2019.02.002>
- Ferrari MD, Goadsby PJ, Burstein R, Kurth T, Ayata C, Charles A et al (2022) Migraine Nat Rev Dis Primers 8(1):2. <https://doi.org/10.1038/s41572-021-00328-4>
- Wang F, Jiang W, Gao L, Liu C, Deng M, Ren X et al (2021) Detecting abnormal neuronal activity in a chronic migraine model by Egr1-EGFP transgenic mice. *Front Neurosci* 15:705938. <https://doi.org/10.3389/fnins.2021.705938>
- Li A, Gong H, Zhang B, Wang Q, Yan C, Wu J et al (2010) Micro-optical sectioning tomography to obtain a high-resolution atlas of the mouse brain. *Science* 330(6009):1404–1408. <https://doi.org/10.1126/science.1191776>
- Yang X, Zhang Q, Huang F, Bai K, Guo Y, Zhang Y et al (2018) High-throughput light sheet tomography platform for automated fast imaging of whole mouse brain. *J Biophotonics* 11(9):e201800047. <https://doi.org/10.1002/jbio.201800047>
- Konno A, Hirai H (2020) Efficient whole brain transduction by systemic infusion of minimally purified AAV-PHP:eB. *J Neurosci Methods* 346:108914. <https://doi.org/10.1016/j.jneumeth.2020.108914>
- Silva BA, Burns AM, Graff J (2019) A cFos activation map of remote fear memory attenuation. *Psychopharmacology* 236(1):369–381. <https://doi.org/10.1007/s00213-018-5000-y>
- Pan Q, Wang Y, Tian R, Wen Q, Qin G, Zhang D et al (2022) Sphingosine-1 phosphate receptor 1 contributes to central sensitization in recurrent nitroglycerin-induced chronic migraine model. *J Headache Pain* 23(1):25. <https://doi.org/10.1186/s10194-022-01397-w>
- Faul F, Erdfelder E, Lang AG, Buchner A (2007) G*Power 3: a flexible statistical power analysis program for the social, behavioral, and biomedical sciences. *Behav Res Methods* 39(2):175–191. <https://doi.org/10.3758/bf03193146>
- Pradhan AA, Smith ML, McGuire B, Tarash I, Evans CJ, Charles A (2014) Characterization of a novel model of chronic migraine. *Pain* 155(2):269–274. <https://doi.org/10.1016/j.pain.2013.10.004>
- Xie W, Li R, Tang W, Ma Z, Miao S, Li C et al (2023) Proteomics profiling reveals mitochondrial damage in the thalamus in a mouse model of chronic migraine. *J Headache Pain* 24(1):122. <https://doi.org/10.1186/s10194-023-01646-6>
- Christensen SL, Munro G, Petersen S, Shabir A, Jansen-Olesen I, Kristensen DM et al (2020) ATP sensitive potassium (K(ATP)) channel inhibition: a promising new drug target for migraine. *Cephalalgia* 40(7):650–664. <https://doi.org/10.1177/0333102420925513>
- Christensen SL, Rasmussen RH, Ernstsens C, La Cour S, David A, Chaker J et al (2021) CGRP-dependent signalling pathways involved in mouse models of GTN- cilostazol- and levromakalim-induced migraine. *Cephalalgia* 41(14):1413–1426. <https://doi.org/10.1177/03331024211038884>
- Christensen SL, Hansen RB, Storm MA, Olesen J, Hansen TF, Ossipov M et al (2020) Von Frey testing revisited: Provision of an online algorithm for improved accuracy of 50% thresholds. *Eur J Pain* 24(4):783–790. <https://doi.org/10.1002/ejp.1528>
- Yang DG, Gao YY, Yin ZQ, Wang XR, Meng XS, Zou TF et al (2023) Roxadustat alleviates nitroglycerin-induced migraine in mice by regulating HIF-1alpha/NF-kappaB/inflammation pathway. *Acta Pharmacol Sin* 44(2):308–320. <https://doi.org/10.1038/s41401-022-00941-3>
- Markovics A, Kormos V, Gaszner B, Lashgarara A, Szoke E, Sandor K et al (2012) Pituitary adenylate cyclase-activating polypeptide plays a key role in nitroglycerol-induced trigeminovascular activation in mice. *Neurobiol Dis* 45(1):633–644. <https://doi.org/10.1016/j.nbd.2011.10.010>
- Louter MA, Pijpers JA, Wardenaar KJ, van Zwet EW, van Hemert AM, Zitman FG, Ferrari MD, Penninx BW, Terwindt GM (2015) Symptom dimensions of affective disorders in migraine patients. *J Psychosom Res* 79(5):458–463. <https://doi.org/10.1016/j.jpsy.2015.05.001>
- Zhang M, Liu Y, Zhao M, Tang W, Wang X, Dong Z, Yu S (2017) Depression and anxiety behaviour in a rat model of chronic migraine. *J Headache Pain* 18(1):27. <https://doi.org/10.1186/s10194-017-0736-z>
- Kooshki R, Abbasnejad M, Esmaeli-Mahani S, Raouf M, Sheibani V (2020) Activation orexin 1 receptors in the ventrolateral periaqueductal gray matter attenuate nitroglycerin-induced migraine attacks and calcitonin gene related peptide up-regulation in trigeminal nucleus caudalis of rats. *Neuropharmacology* 178:107981. <https://doi.org/10.1016/j.neuropharm.2020.107981>
- Cai G, Lu Y, Chen J, Yang D, Yan R, Ren M et al (2022) Brain-wide mapping of c-Fos expression with fluorescence micro-optical sectioning tomography in a chronic sleep deprivation mouse model. *Neurobiol Stress* 20:100478. <https://doi.org/10.1016/j.jynstr.2022.100478>
- Li C, Li Y, Zhang W, Ma Z, Xiao S, Xie W et al (2023) Dopaminergic projections from the hypothalamic A11 nucleus to the spinal trigeminal nucleus are involved in bidirectional migraine modulation. *Int J Mol Sci* 24(23). <https://doi.org/10.3390/ijms242316876>
- Zeng X, Niu Y, Qin G, Zhang D, Chen L (2023) Dysfunction of inhibitory interneurons contributes to synaptic plasticity via GABABR-pNR2B signaling in a chronic migraine rat model. *Front Mol Neurosci* 16. <https://doi.org/10.3389/fnmol.2023.1142072>
- Pi C, Tang W, Li Z, Liu Y, Jing Q, Dai W et al (2022) Cortical pain induced by optogenetic cortical spreading depression: from whole brain activity mapping. *Mol Brain* 15(1). <https://doi.org/10.1186/s13041-022-00985-w>
- Tang C, Unekawa M, Shibata M, Tomita Y, Izawa Y, Sugimoto H et al (2020) Characteristics of cortical spreading depression and c-Fos expression in transgenic mice having a mutation associated with familial hemiplegic migraine 2. *Cephalalgia* 40(11):1177–1190. <https://doi.org/10.1177/0333102420929028>
- He L, Chen N, Su W, Cui S-H, Guo J, Duan J-C et al (2019) A novel large animal model of recurrent migraine established by repeated administration of inflammatory soup into the dura mater of the rhesus monkey. *Neural Regeneration Res* 14(1). <https://doi.org/10.4103/1673-5374.243715>
- Bhatt DK, Ramachandran R, Christensen SLT, Gupta S, Jansen-Olesen I, Olesen J (2014) CGRP infusion in unanesthetized rats increases expression of c-Fos in the nucleus tractus solitarius and caudal ventrolateral medulla, but not in the trigeminal nucleus caudalis. *Cephalalgia* 35(3):220–233. <https://doi.org/10.1177/0333102414535995>
- Bohár Z, Fejes-Szabó A, Tar L, Varga H, Tajti J, Párdutz Á et al (2013) Evaluation of c-Fos immunoreactivity in the rat brainstem nuclei relevant in migraine pathogenesis after electrical stimulation of the trigeminal ganglion. *Neurosci Sci* 34(9):1597–1604. <https://doi.org/10.1007/s10072-013-1292-1>

34. Ter Horst GJ, Meijler WJ, Korf J, Kemper RH (2001) Trigeminal nociception-induced cerebral Fos expression in the conscious rat. *Cephalalgia* 21(10):963–975. <https://doi.org/10.1046/j.1468-2982.2001.00285.x>
35. Zhang C, Yan C, Ren M, Li A, Quan T, Gong H et al (2017) A platform for stereological quantitative analysis of the brain-wide distribution of type-specific neurons. *Sci Rep* 7(1):14334. <https://doi.org/10.1038/s41598-017-14699-w>
36. Quan T, Zheng T, Yang Z, Ding W, Li S, Li J et al (2013) NeuroGPS: automated localization of neurons for brain circuits using L1 minimization model. *Sci Rep* 3:1414. <https://doi.org/10.1038/srep01414>
37. Jia Z, Yu S (2017) Grey Matter alterations in migraine: a systematic review and meta-analysis. *Neuroimage Clin* 14:130–140. <https://doi.org/10.1016/j.nicl.2017.01.019>
38. May A, Ashburner J, Buchel C, McGonigle DJ, Friston KJ, Frackowiak RS et al (1999) Correlation between structural and functional changes in brain in an idiopathic headache syndrome. *Nat Med* 5(7):836–838. <https://doi.org/10.1038/10561>
39. Gan Z, Gangadharan V, Liu S, Korber C, Tan LL, Li H et al (2022) Layer-specific pain relief pathways originating from primary motor cortex. *Science* 378(6626):1336–1343. <https://doi.org/10.1126/science.add4391>
40. Zhu Y, Dai L, Zhao H, Ji B, Yu Y, Dai H et al (2021) Alterations in effective connectivity of the Hippocampus in Migraine without Aura. *J Pain Res* 14:3333–3343. <https://doi.org/10.2147/JPR.S327945>
41. Chattarji S, Tomar A, Suvrathan A, Ghosh S, Rahman MM (2015) Neighborhood matters: divergent patterns of stress-induced plasticity across the brain. *Nat Neurosci* 18(10):1364–1375. <https://doi.org/10.1038/nn.4115>
42. Liu HY, Chou KH, Lee PL, Fuh JL, Niddam DM, Lai KL et al (2017) Hippocampus and amygdala volume in relation to migraine frequency and prognosis. *Cephalalgia* 37(14):1329–1336. <https://doi.org/10.1177/0333102416678624>
43. Stankewitz A, May A (2011) Increased limbic and brainstem activity during migraine attacks following olfactory stimulation. *Neurology* 77(5):476–482. <https://doi.org/10.1212/WNL.0b013e318227e4a8>
44. Lu J, Zhang Z, Yin X, Tang Y, Ji R, Chen H et al (2022) An entorhinal-visual cortical circuit regulates depression-like behaviors. *Mol Psychiatry* 27(9):3807–3820. <https://doi.org/10.1038/s41380-022-01540-8>
45. Ronaghi A, Zibaii MI, Pandamooz S, Nourzei N, Motamedi F, Ahmadiani A et al (2019) Entorhinal cortex stimulation induces dentate gyrus neurogenesis through insulin receptor signaling. *Brain Res Bull* 144:75–84. <https://doi.org/10.1016/j.brainresbull.2018.11.011>
46. Li Z, Zhou J, Lan L, Cheng S, Sun R, Gong Q, Wintermark M, Zeng F, Liang F (2020) Concurrent brain structural and functional alterations in patients with migraine without aura: an fMRI study. *J Headache Pain* 21(1):141. <https://doi.org/10.1186/s10194-020-01203-5>
47. Brodsky JR, Mejico LJ, Giraud A, Woods CI 3rd (2013) Impairment of habituation of the auditory brain stem response in migrainous vertigo. *Ann Otol Rhinol Laryngol* 122(5):308–315. <https://doi.org/10.1177/000348941312200504>
48. He W, Long T, Pan Q, Zhang S, Zhang Y, Zhang D et al (2019) Microglial NLRP3 inflammasome activation mediates IL-1beta release and contributes to central sensitization in a recurrent nitroglycerin-induced migraine model. *J Neuroinflammation* 16(1):78. <https://doi.org/10.1186/s12974-019-1459-7>
49. Wen Q, Wang Y, Pan Q, Tian R, Zhang D, Qin G et al (2021) MicroRNA-155-5p promotes neuroinflammation and central sensitization via inhibiting SIRT1 in a nitroglycerin-induced chronic migraine mouse model. *J Neuroinflammation* 18(1):287. <https://doi.org/10.1186/s12974-021-02342-5>
50. DaSilva AF, Granziera C, Tuch DS, Snyder J, Vincent M, Hadjikhani N (2007) Interictal alterations of the trigeminal somatosensory pathway and periaqueductal gray matter in migraine. *NeuroReport* 18(4):301–305. <https://doi.org/10.1097/WNR.0b013e32801776bb>
51. Sexton PM, McKenzie JS, Mendelsohn FA (1988) Evidence for a new subclass of calcitonin/calcitonin gene-related peptide binding site in rat brain. *Neurochem Int* 12(3):323–335. [https://doi.org/10.1016/0197-0186\(88\)90171-4](https://doi.org/10.1016/0197-0186(88)90171-4)
52. McLatchie LM, Fraser NJ, Main MJ, Wise A, Brown J, Thompson N et al (1998) RAMPs regulate the transport and ligand specificity of the calcitonin-receptor-like receptor. *Nature* 393(6683):333–339. <https://doi.org/10.1038/30666>
53. Wattiez AS, Sowers LP, Russo AF (2020) Calcitonin gene-related peptide (CGRP): role in migraine pathophysiology and therapeutic targeting. *Expert Opin Ther Targets* 24(2):91–100. <https://doi.org/10.1080/14728222.2020.1724285>

Publisher's Note

Springer Nature remains neutral with regard to jurisdictional claims in published maps and institutional affiliations.